Carbohydrate Polymers 84 (2011) 781–787

Contents lists available at ScienceDirect

Carbohydrate Polymers

journal homepage: www.elsevier.com/locate/carbpol

Preparation, characterization and application of superparamagnetic iron oxide encapsulated with N-[(2-hydroxy-3-trimethylammonium) propyl] chitosan chloride

Chia-Rui Shen[a,b,*], Jyuhn-Huarng Juang[c], Zei-Tsan Tsai[b], Shu-Ting Wu[a], Fu-Yuan Tsai[d], Jiun-Jie Wang[b,e], Chao-Lin Liu[f], Tzu-Chen Yen[b,e]

[a] Department of Medical Biotechnology and Laboratory Science, Chang Gung University, Taoyuan, Taiwan
[b] Molecular Imaging Center, Chang Gung Memorial Hospital, Taoyuan, Taiwan
[c] Division of Endocrinology and Metabolism, Department of Internal Medicine, Chang Gung University and Chang Gung Memorial Hospital, Taoyuan, Taiwan
[d] General Education Center, Chang Gung University, Taoyuan, Taiwan
[e] Department of Medical Imaging and Radiological Sciences, Chang Gung University, Taoyuan, Taiwan
[f] Graduate School of Biochemical Engineering and Department of Chemical Engineering, Ming Chi University of Technology, Taipei, Taiwan

ARTICLE INFO

Article history:
Received 8 October 2009
Received in revised form 10 May 2010
Accepted 29 July 2010
Available online 14 August 2010

Keywords:
Cell tracking
Chitosan
Ferrofluid
N-[(2-hydroxy-3-trimethylammonium) propyl] chitosan chloride (HTCC)
Islet transplantation
Magnetic resonance image
Superparamagnetic iron oxide nanocrystals (SPION)

ABSTRACT

Superparamagnetic iron oxide nanocrystals (SPION) and their colloidal solutions of magnetic nanoparticles (ferrofluid) appear to contribute to the magnetite imaging applications. Here we present an aqueous ferrofluid in physiological pH and its cell tracking potential. *In situ* coating method was adapted to synthesize N-[(2-hydroxy-3-trimethylammonium) propyl] chitosan chloride (HTCC)-coated SPION. Characterization results reveal their features as follows: (1) *z*-average diameter of 274.1 ± 1.934 nm; (2) polydispersity index (PDI) of 0.135 ± 0.029; (3) zeta potential of 11.4 ± 0.410 mV; (4) iron concentration of 5.4 mg Fe/ml; (5) stable in both water and normal saline; (6) uptake by a variety of cell lines and (7) little cytotoxicity. Finally, islet grafting experiments demonstrated the potential usefulness of this product as a MRI contrast agent for cell tracking.

1. Introduction

The unique characteristics of molecular imaging, being non-invasive, quantitative, and repetitive imaging of targeted macromolecules and biological processes in living organisms (Herschman, 2002), have recently attracted widespread interests (Deroose, Reumers, Debyser, & Baekelandt, 2009; Jadvar, 2009; Liu et al., 2010; Oates, Gorfinkiel, González-Gaitán, & Heisenberg, 2009; Rudin, 2009). In particular, superparamagnetic iron oxide nanoparticles (SPION) have demonstrated their utility as an important tool for enhancing magnetic resonance contrast (Hirokawa et al., 2009; Huang et al., 2009; Liu et al., 2009b; Medarova & Moore, 2008; Müller, 2009; Theorek, Chen, Czupryna, & Tsourkas, 2006). The use of SPION has made it possible of the combination of the high spatial resolution of magnetic resonance (MR) imaging with the high specificity of magnetic markers (Inoue et al., 2008; Medarova & Moore, 2008; Shieh et al., 2005; Theorek et al., 2006). The cells via phagocytosis or endocytosisof SPION (Metz et al., 2004) present an intracellular magnetic marker (Huang et al., 2009; Islam & Josephson, 2009; Long, van Laarhoven, Bulte, & Levitsky, 2009; Matuszewski et al., 2005; Tsai et al., 2010), resulting in a contrast in MR images by reducing T2.

SPION typically consist of two components, an iron oxide core and a hydrophilic coating. The SPION core can be composed of Fe_3O_4 and/or γ Fe_2O_3. To prevent the presence of free iron oxide, macromolecules are used as coating agent, especially in polysaccharides polymers (Bhattarai, Remant Bahadur, Aryal, Khil, & Kim, 2007; Saboktakin, Maharramov, & Ramazanov, 2009; Somsook et al., 2005; Theorek et al., 2006; Tsai et al., 2010), such as dextran, starch and chitosan. Chitosan is the N-deacetylated product of chitin, one of the most abundant polysaccharide in nature. Chitosan

* Corresponding author at: Department of Medical Biotechnology and Laboratory Science, Chang Gung University, 259 Wen-Hwa 1st Road, Kwei-Shan, Tao-Yuan 333, Taiwan. Tel.: +886 32118800x5200; fax: +886 32118698.
E-mail address: crshen@mail.cgu.edu.tw (C.-R. Shen).

0144-8617/$ – see front matter © 2010 Elsevier Ltd. All rights reserved.
doi:10.1016/j.carbpol.2010.07.067

and its derivatives have been applied widely (Chen, Wang, Liu, & Wang, 2008; Chen, Shen, & Liu, 2010; Don, King, Chiu, & Peng, 2006; Lim & Hudson, 2004; Liu et al., 2009a; Yang et al., 2009) due to its non-toxicity, biocompatibility, and biodegradability. It particularly attracts interests in metal nanoparticles synthesis due to its interaction with metal atoms, metal ions and metal oxide nanoparticles for their stabilization in colloidal suspension (Somsook et al., 2005; Varma, Deshpande, & Kennedy, 2004). Chelation evenly disperses metal oxides throughout chitosan polymer. In this regard, chitosan has been a good dispersant for a variety of different nanoparticles (Ding, Hao, Xue, & Ju, 2007; Huang & Yang, 2004; Peng et al., 2008; Zhu, Yuan, & Liao, 2008) including single-walled carbon nanotubes, gold, and silver nanoparticles, as well as SPION.

Among a number of different synthetic methods to prepare iron oxide nanoparticles, co-precipitation from aqueous Fe^{2+}/Fe^{3+} salt solutions by the addition of a base, is a facile and convenient way (Massart, 1981; Molday & MacKenzie, 1982; Theorek et al., 2006; Tsai et al., 2010). For chitosan and/or its derivatives either only post-synthesis coating method or with addition of crosslinking agent such as glutaraldehyde after post-synthesis coating were employed (Conti, Modena, Genta, Perugini, & Pavanetto, 1998; Hamidi, Azadi, & Rafiei, 2008; Theorek et al., 2006). The pendants on chitosan derivatives were O-carboxymethyl, N-succinyl, N-trimethyl, or N-succinyl-O-carboxymethyl (Don et al., 2006; Lim & Hudson, 2004; Sahni, Chopra, Ahmad, & Khar, 2008; Xu, Du, Huang, & Gao, 2003; Yan, Chen, Gu, & Qin, 2006; Yin, Fei, Cui, Tang, & Yin, 2007). For *in vivo* applications as magnetic resonance imaging (MRI) contrast agent, a colloidally dispersed magnetic nanoparticles (so called ferrofluid) stable at neutral pH is highly desire. However, usually at low pH (less than about 6), chitosan's amines are protonated and positively charged (100% protonation when pH less than 3.4), and chitosan is a water-soluble cationic polyelectrolyte. At higher pH (above about 6.5), chitosan's amines are deprotonated and lose its charge and becomes insoluble. Also, at higher pH, chitosan can undergo interpolymer associations that can lead to fiber and network (i.e. film and gel) formation.

Recently, the Edmonton Protocol has markedly improved the success rate of human islet transplantation (Shapiro et al., 2000). However, long-term function of the transplanted islets has been disappointed; only 10% of patients maintain insulin independence 5 years after transplantation although 80% of patients were C-peptide positive (Ryan et al., 2005). To better understand the fate of transplanted islets, a magnetic resonance imaging (MRI) technique has been used to detect Feridex-labeled transplanted islets in rodents (@@Gilad et al., 2008; Jirak et al., 2004; Medarova and Moore, 2009). Here we utilized a quaternized chitosan, N-[(2-hydroxy-3-trimethylammonium) propyl] chitosan chloride (HTCC), which is one of the water-soluble chitosan and shows better hydroscopic property, moisture retentiveness, mucoadhesivity and permeability enhancing property, comparing with chitosan (Lim and Hudson, 2004; Sahni et al., 2008; Xu et al., 2003). The chemical co-precipitation (so called *in situ* coating) method was adapted to synthesize HTCC -coated superparamagnetic iron oxide nanoparticles. The as-prepared ferrofluid was further characterized for the general features. MRI and cell experiments demonstrated the potential usefulness of this product as a potential MRI contrast agent that might be used for cell tracking.

2. Materials and methods

2.1. Materials

Iron(III) chloride hexahydrate ($FeCl_3{\cdot}6H_2O$) and D-mannitol were obtained from Riedel-de Haen (Germany). Iron(II) chloride tetrahydrate ($FeCl_2{\cdot}4H_2O$) was from Showa (Japan). Ammonium hydroxide solution (25%) was obtained from Fluka (Germany). Low molecular weight chitosan and glycidytrimethylammonium chloride (GTMAC) were from Aldrich (USA). Solid chitosan was subjected to Co-60 γ-ray irradiation at dose of 300 kGy prior to use as described previously (Tsai et al., 2010).

2.2. Preparation of N-[(2-hydroxy-3-trimethylammonium) propyl] chitosan chloride (HTCC)

The chemical structure of HTCC is shown in Fig. 1. It was synthesized by a modified method with the addition of glycidytrimethylammonium chloride (GTMAC) to chitosan (Xu et al., 2003).

2.3. Synthesis of SPION

The chemical co-precipitation method as published elsewhere (Tsai et al., 2010) was adapted to synthesize HTCC-coated superparamagnetic iron oxide nanoparticles (SPION). Briefly, about 0.62 g HTCC was dissolved in 100 ml 0.5% (v/v) aqueous acetic acid. 1 g $FeCl_3{\cdot}6H_2O$ and 0.45 g $FeCl_2{\cdot}4H_2O$ were added to the HTCC solution to get a pale brown solution. Then 15 ml 29% ammonia water was rapidly added to the brown solution under sonication at 50 °C and sonicated further for 40 min. The black precipitate was isolated with a magnet and decanting or centrifugation at 5000 rpm for 5 min and washed with 95% ethanol at least three times till no appearance of AgCl cloud. The washed black precipitate was effected to ferrofluid (an aqueous sol of complex HTCC with SPION) when dispersed in 50 ml water and the pH was adjusted to about 7.0 with lactic acid and the addition of mannitol. The ferrofluid and its stability were characterized with measuring *z*-average diameter (defined as the intensity-weighted average hydrodynamic diameter of the particles being measured) and zeta potential by laser light—scattering apparatus (Zetasizer Nano ZS, Malvern Instruments Ltd., UK). The iron concentration of ferrofluid was photometrically determined using o-phenanthroline and the absorbance was read at 510 nm.

2.4. Cell culture and SPION loading

A variety of cell lines including NIT-1, beta-TC6, alpha-TC1-clone 9, THP-1, K562 cells and primary murine peritoneal cells were utilized for cellular loading of SPION. The cells ($5–10 \times 10^4$ cells/well) in complete medium were seeded in each well of the 24-well plates, and incubated at 37 °C with a 5% CO_2 atmosphere for 16 h. At this time point, the cells were fed with desired doses of SPION for different culture periods as study designed. After washing to remove the excess of iron particles, the iron content within cells was assessed by Prussian blue staining (5% potassium ferrocyanide and 5% HCl were 1:1 mixed for 30 min).

2.5. Cytotoxicity assay

The fluorescence of propidium iodide (PI), which enters exclusively damaged cells, was used to determine the cell death as published elsewhere (Jones & Senft, 1985).

2.6. Transmission electron microscopy

SPION co-cultured cells were fixed in 2.5% glutaraldehyde and postfixed in 1% osmium tetraoxide. They were then dehydrated by alcohol and embedded in epoxy resin for sectioning. Ultra-thin sections were stained with uranyl acetate and lead citrate and examined with a Hitachi H-7500 electron microscope.

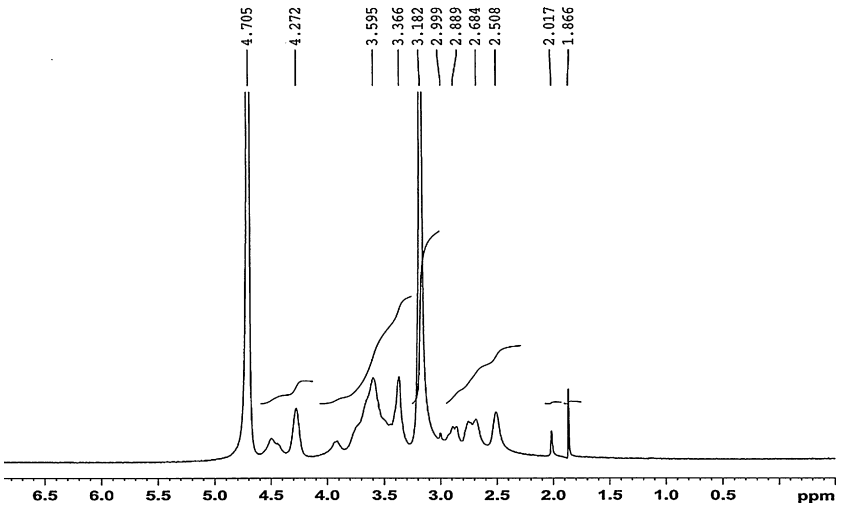

Fig. 1. The chemical structure of N-[(2-hydroxy-3-trimethylammonium) propyl] chitosan chloride (HTCC).

2.7. In vitro MRI study

Magnetic resonance imaging was performed with a 3T scanner (Siemens, Erlangen, Germany) using a surface coil made manually. T2 weighted images were acquired by a Turbo Spin Echo sequence with fat saturation, using a TE/TR of 112 ms/2500 ms. The field of view is 100 mm × 100 mm, with a matrix size of 320 × 320 and a slice thickness of 1 mm. The number of averages is 9, which leads to a total acquisition time of approximately 18 min 20 s. Relaxation measurements were made on samples of HTCC-SPION, SPION loaded and unloaded cells prepared by mixing a cell pellet containing 10^6 cells with 2 ml agarose (3% w/w).

2.8. In vivo islet grafting and MRI study

The animal experiments were approved by the institutional animal ethics committee. Under anesthesia with sodium amobarbital, pancreases of male inbred C57BL/6 mice, aged 8–12 weeks, were distended with 2.5 ml of RPMI-1640 medium (GIBCO BRL, Grand Island, NY, USA) containing 1.5 mg/ml of collagenase (collagenase from Clostridium histolyticum, type XI, Sigma Immunochemicals), excised and incubated in a water bath at 37 °C. The islets were separated by a density gradient (Histopaque-1077; Sigma Immunochemicals), and purified islets were then handpicked under a dissecting microscope (Juang, Hsu, Kuo, & Yao, 2001). After loading with SPION (10 mg/ml) overnight, three hundred islets were syngeneically transplanted under left kidney capsule of each mouse. To accomplish this, the islets were centrifugated in PE-50 tubing (Clay Adams, Parsippany, NJ) connected to a 200-μl pipette tip. With the mouse under amobarbital anesthesia, the left kidney was exposed through a lumbar incision. A capsulotomy was performed in the lower pole of the kidney and the tip of the tubing advanced under the capsule of the upper pole, the site of final injection. The capsulotomy was left unsutured (Juang et al., 2001). After transplantation, serial MR imaging of the recipients were performed 1 week later. Images were acquired on a 3.0 T MR scanner (Magnetom Trio with TIM, Siemens, Erlangen, Germany) using a home-made surface coil. A T2 weighted Turbo Spin Echo sequence was acquired for all subjects.

3. Results and discussions

3.1. Synthesis of SPION encapsulated with HTCC

Magnetite nanoparticles of N-[(2-hydroxy-3-trimethylammonium) propyl] chitosan chloride (HTCC) encapsulating iron oxide were synthesized according to the standard co-precipitation technique, in which iron chloride salts (Fe^{3+} and Fe^{2+}) were directly co-precipitated inside HTCC polymer matrices in an aqueous acetic acid solution. First, the HTCC was synthesized by a modified method with the addition of glycidytrimethylammonium chloride (GTMAC) to chitosan. ^{1}H NMR was utilized to confirm the structure (Fig. 2). Under sonication the iron oxide nanoparticles within polymer matrices were formed

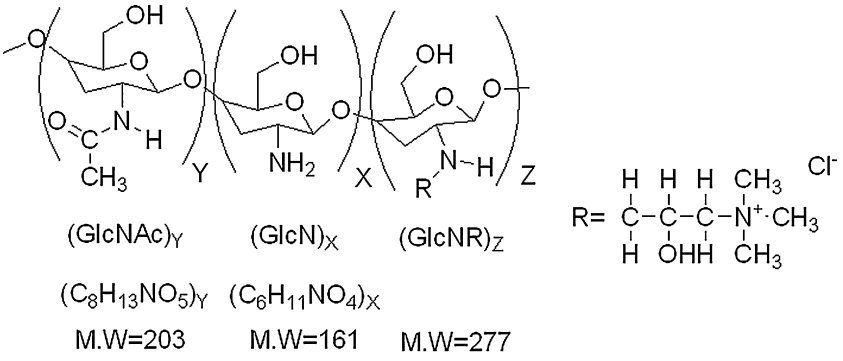

Fig. 2. ^{1}H NMR spectrum of HTCC in de-ionized water.

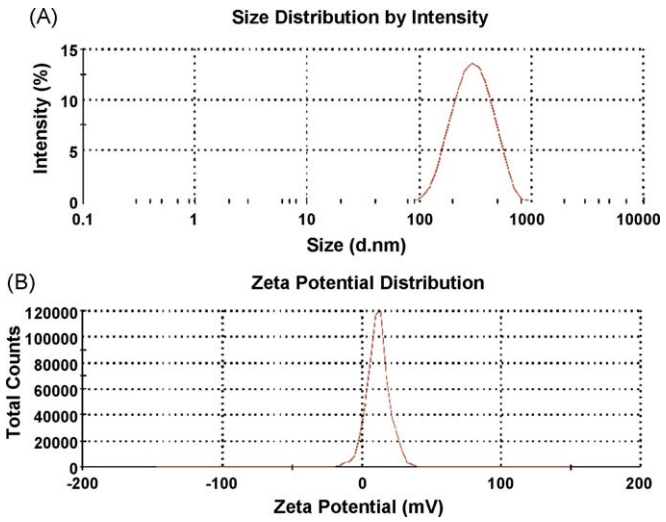

Fig. 3. The (A) size distribution and (B) zeta potential of HTCC-SPION in de-ionized water.

when the pH value subsequently was increased to 9.5 using NH_4OH and the temperature was elevated to 50 °C. The molar ratio for $[Fe^{3+}]$:$[Fe^{2+}]$:$[NH_4OH]$ was 1.6:1:30. The magnetic precipitate was then washed with 95% ethanol till no appearance of AgCl cloud and pH of about 9.0 and separated with centrifugation at 5000 rpm for 5 min. The final ferrofluid (HTCC-SPION) was formed with pH adjustment to about 7.0 with lactic acid and with the addition of mannitol. It appears that the replacement of HTCC might have improved the solubility limitations of conventional chitosan coating of iron oxide nanoparticles and tackles its aqueous solubility at neutral pH.

3.2. Characterization of HTCC-SPION

The HTCC-SPION and its stability were characterized with measuring *z*-average diameter and zeta potential by laser light – scattering apparatus in both water and normal saline solution. The average size of these HTCC-SPION was 274.1 ± 1.934 nm in diameter, carrying a positive zeta potential, 11.4 ± 0.410 mV, in de-ionized water. Fig. 3 shows the results of size distribution (Fig. 3A) and zeta potential (Fig. 3B) of HTCC-SPION in de-ionized water from one representative experiment ($n = 3$). Such results indicate that the as-prepared ferrofluid is with a fairly unimodal distribution of monodisperse clusters. Moreover, the polydispersity index (PDI) and iron content were also determined, and it showed PDI of 0.135 ± 0.029 and iron concentration of 5.4 mg/ml in the as-prepared ferrofluid. The long-term stability study, of which the as-prepared ferrofluid was kept in a variety of solutions at both room temperature and 4 °C and evaluated by measuring the change of *z*-average diameter, revealed that the HTCC-SPION appeared to be stable (data not shown).

In fact, not only in water, we also determined the *z*-average diameter, PDI, and zeta potential of the dissolved HTCC in acetic acid solution and their values were about 150.3 nm and 47.4 mV, respectively, in one representative experiment. It was with the notion that coating with iron oxide, those values mentioned above were changed to somewhat extent. Additionally, it may be questioned whether the substitution percentage of hydrophilic groups affects the features of SPION. The degree of substitution (DS) is defined as the ratio of mole of reacted GTMAC per mole of glucosamine calculated from the original mass of chitosan used. The DS of the HTCC could be measured by titrating the amount of Cl^- ions on the HTCC with aqueous $AgNO_3$ solution. Here, the HTCC with the DS values of 60% appears to be appropriate for encapsulating iron oxide in this study. However, more systemic studies are necessary for further conclusions. Hence, it should be mentioned that once the magnetic precipitate fully dried, it cannot be redispersed to form a stable suspension in water or in acidic solution even with the addition of mannitol.

3.3. Cellular uptake and viability SPION-loaded cells

A variety of cells were utilized to determine the uptake of HTCC-SPION via phagocytosis and endocytosis. It appears that HTCC-SPION could be introduced into all of the cells tested, including the islet cells such as NIT-1, beta-TC6 and alpha-TC1-clone 9, the hematopoietic cells such as THP-1 and K562 cells as well as the primary murine peritoneal cells. Although the levels of SPION uptake might differ among the types of cells, it demonstrated that SPION was found inside the cells by the convenient culture incubation overnight. The intracellular iron content was examined by Prussian blue staining. Fig. 4A gives a representative example of SPION uptake in K562 cells. It shows no blue stain in the control cells without SPION loading. In contrast, the blue color spots (indicating the loaded iron nanoparticles) were mostly located in the cytoplasm although some may present outside the membrane. Transmission electro microscopy (TEM) results confirmed the intracellular location of iron particles. Fig. 4B and C shows the incorporation of the HTCC-SPION particles into phagocytic/endocytic vacuoles of THP and K562 cells. The dense packing of SPION in the cells should, in principle, leads to a large local magnetic field, i.e. one resulting in higher contrast in MR images.

Nonspecific labeling of cell lines, primary cells and stem cells with the magnetic nanoparticles has widely applied in biomedical research (Huang et al., 2009; Inoue et al., 2008; Medarova & Moore, 2008; Theorek et al., 2006). However, targeted loading of these iron oxide nanoparticles appears to be the issues. Although several groups have focused to develop functional group available magnetic nanoparticles (Matuszewski et al., 2005; Shieh et al., 2005; Xu et al., 2003), the availability in the market is still limited. Here, we have developed a formulation of functionalized SPION by encapsulating of these magnetic particles with amine group containing chitosan. This strategy enhances at least three folds the potential of the magnetic nanoparticles for cell tracking. First, the iron oxide moiety helps the magnet-enhanced MR imaging. Second, the improved solubility and stability of these SPION at neutral pH provides convenient and safer candidate of MR contrast agent. Third, targeted properties can be achieved by the amine group of chitosan.

It is always essential to assess cell viability of material before it being used *in vivo*. Here we mainly utilized the fluorescence of propidium iodide (PI), which enters exclusively damaged cells, to determine the cell death. The cells being tested were loaded with serial doses of HTCC-SPION, and assessed for their viability after co-culture for 24 h. Also, to evaluate the duration effects on the cell viability, three different doses, i.e. 2.5, 10 and 40 mg/ml of HTCC-SPION were added in the cultures and the cell viability was assessed after 24, 48, 72 and/or 96 h. Fig. 5 presents one representative results of K562 cells. There was almost no or little, if any, cytotoxicity was found for K562 cells loaded with 2.5, 5, 10, 20, 40 and 80 mg/ml of HTCC-SPION for 24 h (Fig. 5A) as well as for K562 cells with 10 mg/ml for 24, 48 and 72 h (Fig. 5B). Trypan blue exclusion assay also confirmed the results (data not shown).

3.4. In vitro and in vivo MRI studies

The benefit of loading cells by either phagocytosis or endocytosis, which leads to dense packing of a large number of SPION into phagocytic/endocytic vacuoles, is evident from the MR image of a multi-well plate preparation as shown in Fig. 6A. A 12-well culture plate were prepared containing SPION-labeled cells in 3% agarose

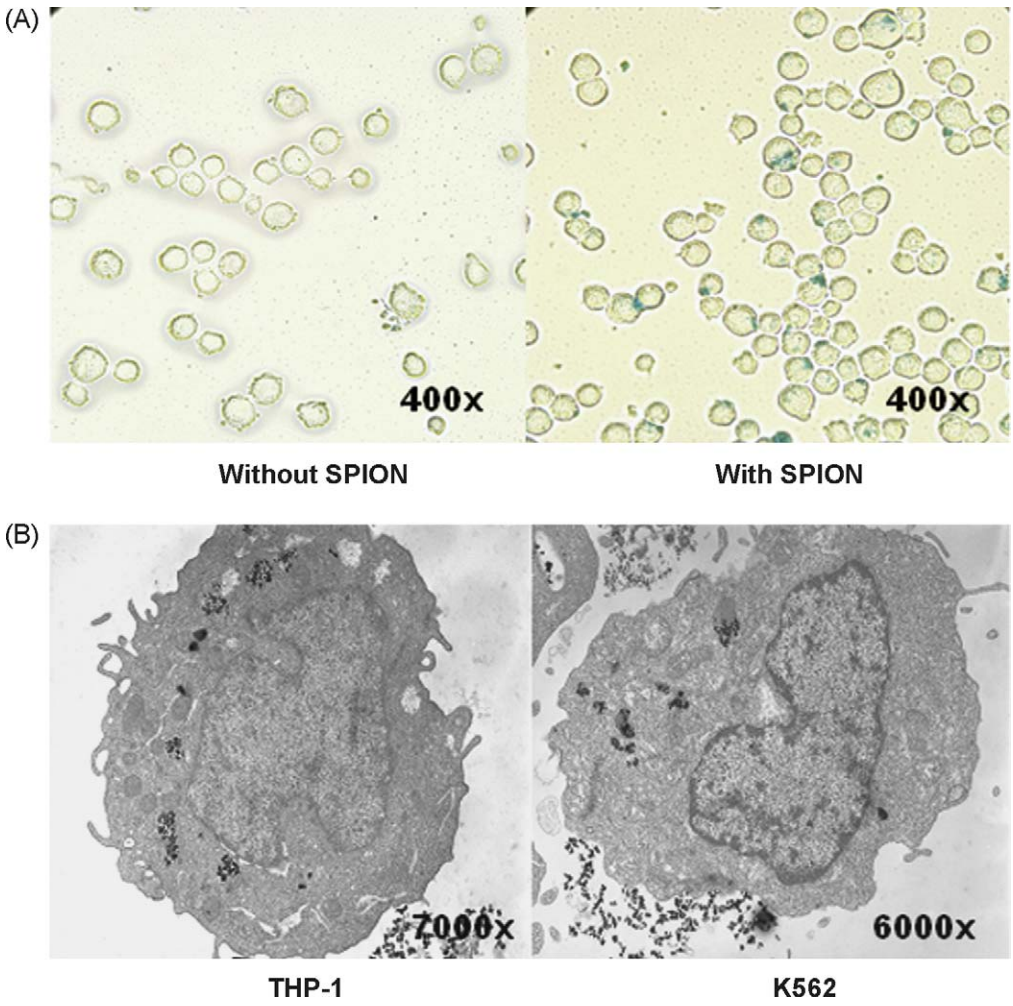

Fig. 4. Cellular iron content assessed by (A) Prussian blue staining of HTCC-SPION loading THP-1 cells, and TEM analysis of (B)THP-1 and (C) K562 cells loaded with HTCC-SPION at 37 °C for 24 h.

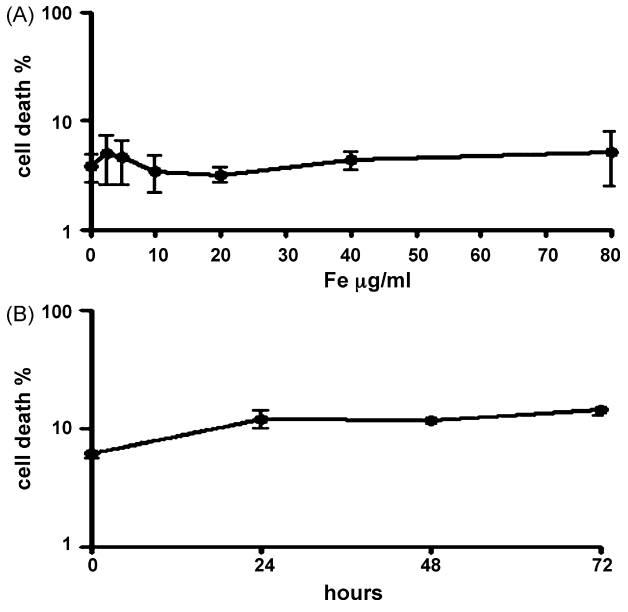

Fig. 5. Effects of (A) a variety dose of HTCC-SPION and (B) reacting period on the viability of ferrofluid loading cells.

and imaged with a 3T scanner (Siemens, Erlangen, Germany) using a surface coil made manually. T2 weighted images were acquired, and it appears that the dark spots in MR images might correspond to the locations of single loaded cells was supported by the good correlation of the measured spot count with that calculated from the sample cell concentration (data not shown). Indeed, Fig. 6A demonstrates that the dark spots were accumulated in the well of SPION loading cells but not the well with cells only.

An always-interesting issue is the cellular uptake efficiency of these magnetic particles. Of note, the uptake of our HTCC-SPION was in a dose- and time-dependent manner assessed by TEM analysis (data not shown). It may be argued that the magnetic property of iron oxide resulted from the magnetic nanoparticles on the cell membrane. Indeed, it happened in some experiments when initially loaded with a large amount of ferrofluid. However, after intensive washing, the loaded nanoparticles were predominately located in the cytoplasm (Fig. 4B), although it was somewhat cell type-dependent, i.e. the loaded SPION were present both on the membrane and in the cytoplasm (Fig. 4C). Therefore, we did not always obtain the excellent correlation of the measured MR signal changes with the sample cell concentration.

Three hundred HTCC-SPION-labeled islets were syngeneically transplanted under left kidney capsule of each mouse using a protocol described previously (Juang et al., 2001). After transplantation, serial MR imaging of the recipients were performed 1 week later. Images were acquired on a 3.0 T MR scanner (Magnetom Trio with

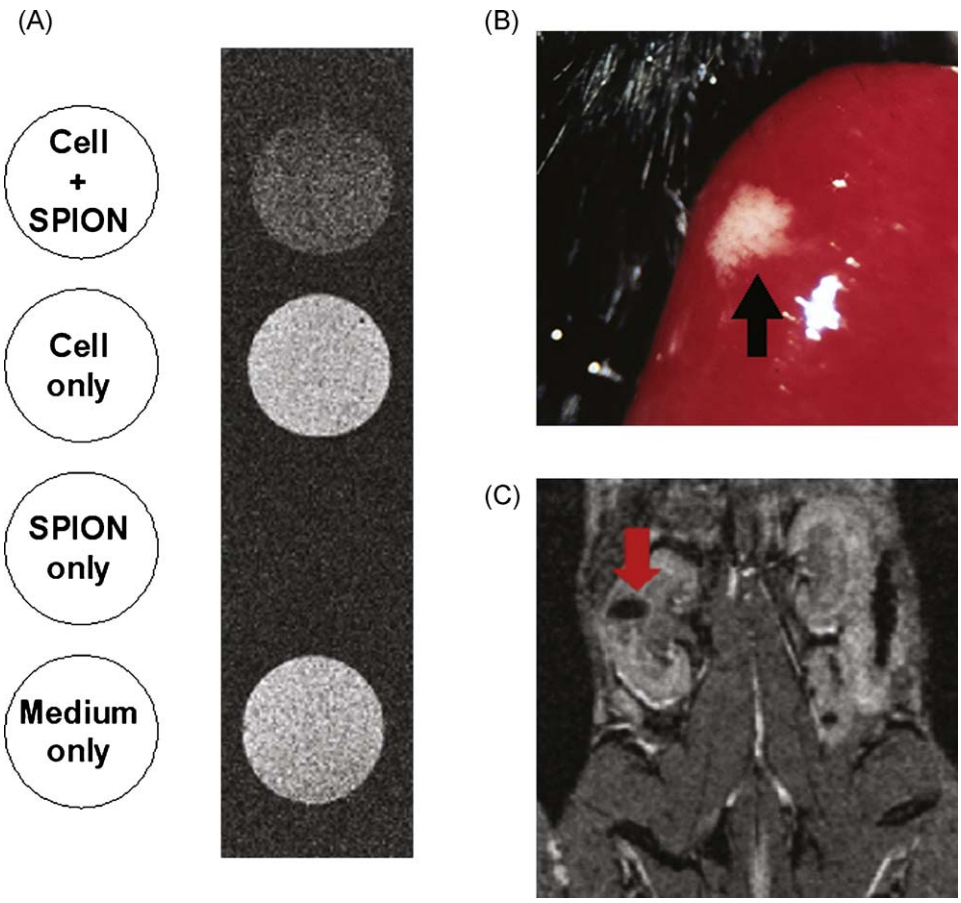

Fig. 6. MRI studies (A) *in vitro* MR image of HTCC-SPION loaded cells, (B) photograph of the grafted islets located upon the kidney, and (C) *in vivo* MR image of grafted islets.

TIM, Siemens, Erlangen, Germany). It can be seen from Fig. 6C that the grafted SPION-labeled islets or islet clusters appeared as dark signal voids in the upper kidney. In fact, the locations of grafted islets were identical from the photographic analysis (Fig. 6B). Hence, the regions of interest were gated on the MR images and their average signal intensities were compared with the regions without SPION-loaded islets in the kidney or the region of muscle (data not shown). It confirms that iron labeled cells appear as regions of signal loss in MR images.

In fact, more and more evidence indicate that the experimental visualization of iron labeled cells *in vivo* with cellular MRI is achievable (Huang et al., 2009; Inoue et al., 2008; Matuszewski et al., 2005; Medarova & Moore, 2008; Shieh et al., 2005; Wu et al., 2006). In fact, since 2004, a number of studies have provided evidence that cellular MRI permits the detection and monitoring of grafted islets *in vivo* (Jirak et al., 2004; Medarova & Moore, 2008). More specifically, the cellular tagging with SPION permits the non-invasive way to directly assess the transplanted islets distribution and survival, which could be used to evaluate the proposed interventions on islet graft loss and modifications of immunosuppressive strategy. However, the challenges may exist due to the low iron content of SPION loading islets and/or the limited availability of the high field MRI instrument. Furthermore, Feridex, which was used usually for labeling of the islet graft, was off market, thus it never doubt that an alternative aqueous ferrofluid are essential.

Another issue might be raised is the toxicity and the degradability of these magnetic particles *in vivo*. Here chitosan, the encapsulating substance for these iron oxide, was selected due to its well known non-toxic and good biocompatibility. We have noted the longer retention and being non-toxic of our HTCC-SPION upto 4 months in islet transplantation experiments (data not shown). It indicates the safety and utility of as-prepared ferrofluid. Additionally, some unlabeled cells were found in the SPION loading islets (data not shown). It appears that different cell types may have a variety of HTCC-SPION uptake efficiency and capacity. Moreover, although such cells do not contribute to MR images, they may play roles in maintaining islet survival or function. Therefore, more studies are necessary to characterize the islet cells with different capabilities to internalize SPION and we cannot simply neglect the alternative approach to label islets or other cells.

4. Conclusion

In this study, we have prepared and evaluated the soluble HTCC-SPION as a novel T2 contrast agent for labeling islet grafts. Such SPION has been characterized and further demonstrated its low cytotoxicity and intracellular uptake by loading to cells. After transplantation, the grafted islet was visualized by a clinical conventional MRI. This permits the detection of graft cells or tissues by MRI to study the graft localization and posttransplant fate *in vivo*.

Conflict of interest

No competing financial interests exist.

Acknowledgements

CRS, JHJ and ZTT contributed equally to this work. This study was financially supported in part by the Chang Gung Memorial Hospi-

tal Grant CMRPD150382 to CRS, CMRPG370361 and 370871 to JHJ, and CMRPG 360741 to ZTT, and National Science Council grant 98-2320-B-182-014-MY3 to CRS. We gratefully acknowledge the kind technical assistance of Ms. Hsiao-Yun Kuo, Jen-Fei Wang and Yu-Wen Chien and editing help of Ms. Lilian YC Chung and Dr. Ching-Jen Yang.

References

Bhattarai, S. R., Remant Bahadur, K. C., Aryal, S., Khil, M. S., & Kim, H. Y. (2007). *N*-Acylated chitosan stabilized iron oxide nanoparticles as a novel nano-matrix and ceramic modification. *Carbohydrate Polymers*, *69*(3), 467–477.

Chen, C. L., Wang, Y. M., Liu, C. F., & Wang, J. Y. (2008). The effect of water-soluble chitosan on macrophage activation and the attenuation of mite allergen-induced airway inflammation. *Biomaterials*, *29*(14), 2173–2182.

Chen, J. K., Shen, C. R., & Liu, C. L. (2010). N-Acetylglucosamine: Production and applications. *Marine Drugs*, *8*(9), 2493–2516.

Conti, B., Modena, T., Genta, I., Perugini, P., & Pavanetto, F. (1998). A proposed new method for the crosslinking of chitosan microspheres. *Drug Delivery*, *5*(2), 87–93.

Deroose, C. M., Reumers, V., Debyser, Z., & Baekelandt, V. (2009). Seeing genes at work in the living brain with non-invasive molecular imaging. *Current Gene Therapy*, *9*(3), 212–238.

Ding, L., Hao, C., Xue, Y., & Ju, H. (2007). A bio-inspired support of gold nanoparticles-chitosan nanocomposites gel for immobilization and electrochemical study of K562 leukemia cells. *Biomacromolecules*, *8*(4), 1341–1346.

Don, T. M., King, C. F., Chiu, W. Y., & Peng, C. A. (2006). Preparation and characterization of chitosan-g-poly(vinyl alcohol)/poly(vinyl alcohol) blends used for the evaluation of blood-contacting compatibility. *Carbohydrate Polymers*, *63*(3), 331–339.

Gilad, A. A., Walczak, P., McMahon, M. T., Na, H. B., Lee, T. T., Hyeon, T., et al. (2008). MR tracking of transplanted cells with positive contrast using manganese oxide nanoparticles. *Magnetic Resonance of Medicine*, *60*, 1–7.

Hamidi, M., Azadi, A., & Rafiei, P. (2008). Hydrogel nanoparticles in drug delivery. *Advanced Drug Delivery Reviews*, *60*(15), 1638–1649.

Herschman, H. R. (2002). Non-invasive imaging of reporter genes. *Journal of Cellular Biochemistry Supplement*, *39*, 36–44.

Hirokawa, Y., Isoda, H., Maetani, Y. S., Arizono, S., Shimada, K., Okada, T., et al. (2009). Hepatic lesions: Improved image quality and detection with the periodically rotated overlapping parallel lines with enhanced reconstruction technique–evaluation of SPIO-enhanced T2-weighted MR images. *Radiology*, *251*(2), 388–397.

Huang, D. M., Hsiao, J. K., Chen, Y. C., Chien, L. Y., Yao, M., Chen, Y. K., et al. (2009). The promotion of human mesenchymal stem cell proliferation by superparamagnetic iron oxide nanoparticles. *Biomaterials*, *30*(22), 3645–3651.

Huang, H., & Yang, X. (2004). Synthesis of polysaccharide-stabilized gold and silver nanoparticles: A green method. *Carbohydrate Research*, *39*(15), 2627–2631.

Inoue, T., Kudo, M., Hatanaka, K., Takahashi, S., Kitai, S., Ueda, T., et al. (2008). Imaging of hepatocellular carcinoma: Qualitative and quantitative analysis of postvascular phase contrast-enhanced ultrasonography with sonazoid. *Oncology*, *75*(Suppl. 1), 48–54.

Islam, T., & Josephson, L. (2009). Current state and future applications of active targeting in malignancies using superparamagnetic iron oxide nanoparticles. *Cancer Biomark*, *5*(2), 99–107.

Jadvar, H. (2009). Molecular imaging of prostate cancer with 18F-fluorodeoxyglucose PET. *Nature Reviews Urology*, *6*(6), 317–323.

Jirak, D., Kriz, J., Herynek, V., Anderson, B., Girman, P., Burian, M., et al. (2004). MRI of transplanted pancreatic islets. *Magnetic Resonance of Medicine*, *52*, 1228–1233.

Jones, K. H., & Senft, J. A. (1985). An improved method to determine cell viability by simultaneous staining with fluorescein diacetate-propidium iodide. *Journal of Histochemistry & Cytochemistry*, *33*(1), 77–79.

Juang, J. H., Hsu, B. R., Kuo, C. H., & Yao, N. K. (2001). Influence of donor age on mouse islet characteristics and transplantation. *Cell Transplantation*, *10*(3), 277–284.

Lim, S. H., & Hudson, S. M. (2004). Application of a fiber-reactive chitosan derivative to cotton fabric as an antimicrobial textile finish. *Carbohydrate Polymers*, *339*(2), 313–319.

Liu, C. L., Shen, C. R., Hsu, F. F., Chen, J. K., Wu, P. T., Guo, S. H., et al. (2009). Gross ML. Isolation and identification of two novel SDS-resistant secreted chitinases from Aeromonas schubertii. *Biotechnology Progress*, *25*(1), 124–131.

Liu, H. L., Hsu, P. H., Chu, P. C., Wai, Y. Y., Chen, J. C., Shen, C. R., et al. (2009). Magnetic resonance imaging enhanced by superparamagnetic iron oxide particles: Usefulness for distinguishing between focused ultrasound-induced blood-brain barrier disruption and brain hemorrhage. *Journal of Magnetic Resonance Imaging*, *29*(1), 31–38.

Liu, H. L., Wai, Y. Y., Hsu, P. H., Lyu, L. A., Wu, J. S., Shen, C. R., et al. (2010). In vivo assessment of macrophage CNS infiltration during disruption of the blood-brain barrier with focused ultrasound: A magnetic resonance imaging study. *Journal of Cerebral Blood Flow & Metabolism*, *30*, 177–186.

Long, C. M., van Laarhoven, H. W., Bulte, J. W., & Levitsky, H. I. (2009). Magnetovaccination as a novel method to assess and quantify dendritic cell tumor antigen capture and delivery to lymph nodes. *Cancer Research*, *69*(7), 3180–3187.

Massart, R. (1981). Preparation of Aqueous Magnetic Liquids in Alkaline and Acidic Media. *IEEE Transactions on Magnetics*, *171*, 1247–1248.

Matuszewski, L., Persigehl, T., Wall, A., Schwindt, W., Tombach, B., Fobker, M., et al. (2005). Cell tagging with clinically approved iron oxides: Feasibility and effect of lipofection, particle size, and surface coating on labeling efficiency. *Radiology*, *235*(1), 155–161.

Medarova, Z., & Moore, A. (2008). Non-invasive detection of transplanted pancreatic islets. *Diabetes, Obesity and Metabolism*, *10*(Suppl. 4), 88–97.

Metz, S., Bonaterra, G., Rudelius, M., Settles, M., Rummeny, E. J., & Daldrup-Link, H. E. (2004). Capacity of human monocytes to phagocytose approved iron oxide MR contrast agents in vitro. *European Radiology*, *14*(10), 1851–1858.

Molday, R. S., & MacKenzie, D. (1982). Immunospecific ferromagnetic iron-dextran reagents for the labeling and magnetic separation of cells. *Journal of Immunology Methods*, *52*, 353–367.

Müller, R. (2009). Hierarchical microimaging of bone structure and function. *Nature Reviews Rheumatology*, *5*(7), 373–381.

Oates, A. C., Gorfinkiel, N., González-Gaitán, M., & Heisenberg, C. P. (2009). Quantitative approaches in developmental biology. *Nature Reviews Genetics*, *10*(8), 517–530.

Peng, C. C., Yang, M. H., Chiu, W. T., Chiu, C. H., Yang, C. S., Chen, Y. W., et al. (2008). Composite nano-titanium oxide-chitosan artificial skin exhibits strong wound-healing effect-an approach with anti-inflammatory and bactericidal kinetics. *Macromolecular Bioscience*, *8*(4), 316–327.

Rudin, M. (2009). Noninvasive structural, functional, and molecular imaging in drug development. *Current Opinion in Chemical Biology*, *13*(3), 360–371.

Ryan, E. A., Paty, B. W., Senior, P. A., Bigam, D., Alfadhli, E., Kneteman, N. M., et al. (2005). Five-year follow-up after clinical islet transplantation. *Diabetes*, *54*, 2060–2069.

Saboktakin, M. R., Maharramov, A., & Ramazanov, M. A. (2009). Synthesis and characterization of superparamagnetic nanoparticles coated with carboxymethyl starch (CMS) for magnetic resonance imaging technique. *Carbohydrate Polymers*, *78*(2), 292–295.

Sahni, J. K., Chopra, S., Ahmad, F. J., & Khar, R. K. (2008). Potential prospects of chitosan derivative trimethyl chitosan chloride (TMC) as a polymeric absorption enhancer: Synthesis, characterization and applications. *The Journal of Pharmacy and Pharmacology*, *60*(9), 1111–1119.

Shapiro, A. M. J., Lakey, J. R. T., Ryan, E. A., Korbutt, G. S., Toth, E., Warnock, G. L., et al. (2000). Islet transplantation in seven patients with type 1 diabetes mellitus using a glucocorticoid-free immunosuppressive regimen. *New England Journal of Medicine*, *343*, 230–238.

Shieh, D. B., Cheng, F. Y., Su, C. H., Yeh, C. S., Wu, M. T., Wu, Y. N., et al. (2005). Aqueous dispersions of magnetite nanoparticles with NH3+ surfaces for magnetic manipulations of biomolecules and MRI contrast agents. *Biomaterials*, *26*(34), 7183–7191.

Somsook, E., Hinsin, D., Buakhrong, P., Teanchai, R., Mophan, N., Pohmakotr, M., et al. (2005). Interactions between iron(III) and sucrose, dextran, or starch in complexes. *Carbohydrate Polymers*, *61*(3), 281–287.

Theorek, D. L. J., Chen, A. K., Czupryna, J., & Tsourkas, A. (2006). Superparamagnetic iron oxide nanoparticle probes for molecular imaging. *Annals of Biomedical Engineering*, *34*(1), 23–38.

Tsai, Z. T., Wang, J. F., Kuo, H. Y., Shen, C. R., Wang, J. J., & Yen, T. C. (2010). In situ preparation of high relaxivity iron oxide nanoparticle with chitosan coating as potential MRI contrast agent and cell tracking agent. *Journal of Magnetism and Magnetic Materials*, *322*, 208–213.

Varma, A. J., Deshpande, S. V., & Kennedy, J. F. (2004). Metal complexation by chitosan and its derivatives: A review. *Carbohydrate Polymers*, *55*(1), 77–93.

Wu, Y. L., Ye, Q., Foley, L. M., Hitchens, T. K., Sato, K. J., Williams, B., et al. (2006). In situ labeling of immune cells with iron oxide particles: An approaches to detect organ rejection by cellular MRI. *Proceedings of the National Academy of Science*, *103*, 1852–1857.

Xu, Y., Du, Y., Huang, R., & Gao, L. (2003). Preparation and modification of N-(2-hydroxyl) propyl-3-trimethyl ammonium chitosan chloride nanoparticle as a protein carrier. *Biomaterials*, *24*, 5015–5022.

Yan, C., Chen, D., Gu, J., & Qin, J. (2006). Nanoparticles of 5-fluorouracil (5-FU) loaded N-succinyl-chitosan (Suc-Chi) for cancer chemotherapy: Preparation, characterizatio—In vitro drug release and anti-tumour activity. *The Journal of Pharmacy and Pharmacology*, *58*(9), 1177–1181.

Yang, C. J., Liu, Y. K., Liu, C. L., Shen, C. N., Kuo, M. L., Su, C. C., et al. (2009). Inhibition of Acidic Mammalian Chitinase by RNA Interference Suppresses OVA-sensitized Allergic Asthma. *Human Gene Therapy*, *20*, 1597–1606.

Yin, L., Fei, L., Cui, F., Tang, C., & Yin, C. (2007). Superporous hydrogels containing poly(acrylic acid-co-acrylamide)/O-carboxymethyl chitosan interpenetrating polymer networks. *Biomaterials*, *28*(6), 1258–1266.

Zhu, A., Yuan, L., & Liao, T. (2008). Suspension of Fe(3)O(4) nanoparticles stabilized by chitosan and o-carboxymethylchitosan. *International Journal Pharmaceutics*, *350*(1–2), 361–368.